J Mater Sci (2011) 46:5117–5128
DOI 10.1007/s10853-011-5443-6

Processing of concentrated aqueous fluorapatite suspensions by slip casting

María P. Albano · Liliana B. Garrido

Received: 16 November 2010 / Accepted: 5 March 2011 / Published online: 12 March 2011

Abstract In order to produce stable aqueous fluorapatite (FA) suspensions, its surface reactivity in an aqueous solution having two initial pH values with a concentration of ammonium polyacrylate (NH_4PA) was investigated as a function of time. The rheological behaviour of concentrated aqueous FA slips stabilized with NH_4PA was studied; besides, the effect of poly(vinyl)alcohol (PVA) addition on the relative viscosity of the suspensions was investigated. The influence of the slip rheology on the microstructure of the resultant green slip cast compacts and their sintering behaviour were determined. Upon the FA introduction in the aqueous solutions, an initial release of F anions located at the surface was found, which was not dependent on the pH and the presence of dispersant. The increase in the initial pH of the solution above 7 and/or the addition of NH_4PA markedly reduced the Ca^{++}/H^{+} exchange reaction rate. As a result, well-stabilized concentrated aqueous suspensions could be obtained at pH close to 9. The minimum viscosity of 40 vol.% slips at pH 8.9 occurred at 0.6 wt% of NH_4PA added. The addition of 0.5 wt% PVA to a well-stabilized FA slip caused aggregation of particles by a depletion flocculation mechanism, thereby increasing the slip viscosity. The greater permeability of cakes produced from slips with high viscosity values (0.5 wt% PVA) increased the casting rate. The highest sintered densities were obtained for the compacts prepared from the slips without PVA, due to the denser particle packing achieved in the green bodies.

M. P. Albano (✉) · L. B. Garrido
Centro de Tecnología de Recursos Minerales y Cerámica (CETMIC), C.C. 49 (B1897ZCA), M. B. Gonnet, Provincia de Buenos Aires, Argentina
e-mail: palbano@cetmic.unlp.edu.ar

Introduction

Calcium orthophosphates such as fluorapatite ($Ca_{10}(PO_4)_6F_2$) are widely used as bone substitute materials due to their chemical similarity to the mineral component of mammalian bones and teeth [1, 2]. Fluorapatite (FA) is non-toxic, biocompatible, not recognized as foreign material in the body and, most importantly, exhibits bioactive behaviour and integrates into living tissue by the same processes active in remodelling healthy bone. These characteristics lead to an intimate physicochemical bond between the implants and bone, termed osteointegration [3]. Even so, the major limitations to use fluorapatite as load-bearing biomaterials is its mechanical properties, it is brittle with a poor fatigue resistance [4]. The poor mechanical behaviour is even more evident for highly porous ceramics and scaffolds with pore sizes greater than 100 μm (this large pore size is a requirement for proper vascularization and bone cell colonization [5]). That is why, in biomedical applications fluorapatite is used primarily as fillers and coatings. Bioinert ceramic such as porous ZrO_2 can be coated with FA to achieve a high mechanical strength as well as a suitable biocompatibility of the system [6, 7]. A relatively thick FA coating layer on ZrO_2 can be fabricated by dip coating. When a dry porous substrate is dipped into a ceramic suspension and subsequently withdrawn from it, a wet dense cake of well-defined thickness can be formed on the substrate surface. After being dried and sintered, a ceramic membrane is achieved.

The first step in this process is the preparation of stable concentrated FA suspensions with the addition of a

dispersant and a binder. Concentrated FA suspensions based on organic solvents have been prepared [7, 8]. In recent years, environmental protection and safety reasons have induced the replacement of non-aqueous organic solvents for an aqueous media. However, the rheological behaviour of concentrated FA aqueous suspensions has not been studied. Successful colloidal processing of fine ceramic powders requires accurate control of both rheological properties and the state of the dispersion. Anionic polyelectrolytes such as NH_4PA are commonly used as dispersant of ceramic powders in aqueous media [9, 10]. The polyelectrolyte adsorbs at the solid–liquid interface and infers repulsive force between the particles which keeps the particles well dispersed; the repulsive interactions are caused by electrostatic and steric effects [11].

The preparation of stable suspensions in aqueous solution is strongly limited by the solubility of FA, which is rather high in acidic conditions. Little attention has been paid to the study of its surface reactivity in an aqueous solution with NH_4PA in weakly alkaline conditions, at which the anionic polyelectrolyte is dissociated. In order to produce well-stabilized slips, first its surface reactivity in an aqueous solution having two initial pH values with a concentration of NH_4PA was investigated as a function of time.

At high solids loading, relatively low slip viscosity can only be achieved in the presence of an optimum dispersion state of particles. Therefore, the adsorption behaviour of NH_4PA and the influence of NH_4PA addition on the rheological properties of 40 vol.% FA slips were studied. As we have mentioned the binder is an essential component for the effective processing of films on substrates. The binder provides strong adhesion between the ceramic particles and the substrate, preventing the powder from detaching off the substrate during thermal treatment. Poly(vinyl)alcohol (PVA) is frequently used in an aqueous media due to its affinity with the processing liquid. Furthermore, it has an effective burnout profile without the formation of a deleterious residue. However, the addition of the organic binder affects the rheology of the suspension [12, 13]. Therefore, the influence of PVA addition on the relative viscosity of 38 vol.% FA suspensions stabilized with NH_4PA was investigated.

The layer formation process by dip coating is similar to the formation of a cake on a porous mould by slip casting [14], in both the driving force for the liquid flow is the capillary suction pressure of the substrate. The rheological behaviour of the suspensions greatly affects the growth rate of the cake and the resultant green density [15]. Therefore, the casting rate of well-stabilized 38 vol.% FA slips with and without PVA, and the resultant green body microstructure were examined and related to the degree of slip dispersion. Finally, the densification of cast samples obtained from both slips was investigated as a function of the sintering temperature.

Experimental procedure

Materials

The $Ca_3(PO_4)_2$ (Fluka, Germany) and CaF_2 (Sigma-Aldrich, Ireland) powders were mixed in a 3:1.5 ratio; thus, CaF_2 was in excess with respect to the stoichiometric ratio for the reaction

$$3Ca_3(PO_4)_2 + CaF_2 \rightarrow Ca_{10}(PO_4)_6F_2 \quad (1)$$

The mixture of powders was calcined 3 h at 1000 °C. Then, the powder was milled in an attrition mill using 1.6 mm zirconia balls with 0.047 wt% NH_4PA during 48 h. First, distilled water with the pH adjusted at 9 was added to the attrition mill; then the dispersant, thereafter the powder and finally the zirconia balls were added. The powder was added in portions to the suspension and the pH was manually adjusted to be maintained at 9 during the additions. The milled powder was washed with distilled water and dried at 100 °C. This powder subsequently referred as FA was used for the experiments presented in this study.

A commercial ammonium polyacrylate solution (Duramax D 3500, Rohm & Haas, Philadelphia PA) and a 9 wt% PVA solution were used as deflocculant and binder, respectively. The degree of hydrolysis of PVA was 87–89% and the average molecular weight was in the range of 57000–66000 g/mol.

Powder characterization

The specific surface area of the calcined and FA powders was measured by single-point BET (Micromeritics Accusorb, USA). The chemical composition of the powders was determined after alkaline fusion. The infrared spectra (FTIR-ATR) of the calcined and FA powders were obtained with a spectrometer (Perkin Elmer, Espectrum One, USA) using a 4 cm^{-1} resolution over the 4000–650 cm^{-1} region. The crystalline phases in the FA powder were determined by X-ray diffraction (XRD) using a diffractometer Philips (3020 goniometer with PW3710 controler, Cu Kα radiation and Ni filter at 40 kV–20 mA).

FA surface reactivity measurements

In order to estimate the isoelectric point (IEP) of the FA, mean particle diameter measurements of 1.1 vol.% suspensions with 0 and 0.56 wt% NH_4PA at different pH values were developed using a Sedigraph (Micromeritics,

USA). Three suspensions having a FA content of 10.4 vol.% were prepared as follows: (1) FA was added to distilled water, (2) FA was added to distilled water with 0.6 wt% NH_4PA at an initial pH 7.7 and (3) FA was added to an aqueous solution having an initial pH of 8.9 with 0.6 wt% NH_4PA. The aqueous dissolution behaviour of FA was studied by measuring the pH of the suspensions and the Ca/P, F/P atomic ratio in the solid phase, as a function of time for the 1, 2 and 3 slips. The Ca/P and F/P atomic ratios were determined by chemical analysis and energy-dispersive X-ray analysis (SEM-EDX, Philips 505 equipment with EDX accesory) after centrifugalizing the suspensions, washing the powders twice with distilled water and drying them at 100 °C. To aid in the interpretation of solubility measurements the infrared spectra (FTIR-ATR) of the three samples following their dissolution for 17 days and no reacted FA were determined.

Slip preparation

40 vol.% aqueous FA slips with various amounts of deflocculant were prepared by suspending particles in deionized water via 20 min of ultrasound; the pH was manually adjusted to be maintained at 8.9. In addition, 38 vol% suspensions with 0.6 wt% NH_4PA and two PVA concentrations were prepared.

Powder characterization and NH_4PA adsorption measurements

40 vol.% slips with NH_4PA were centrifuged, afterwards the solid was washed with distilled water, dried at 100 °C and analysed by FTIR-ATR. The spectra of this powder were compared with that of FA.

In order to determine the amount of NH_4PA adsorbed, slips were centrifuged for 30 min at 2500 rpm and washed twice with distilled water. Then, the solid was dried at 100 °C and analysed by thermal gravimetric analysis (TGA) (Model STA 409, Netzsch Inc., Germany) at a heating rate of 10 °C/min in air. The TGA data showed a water weight loss at temperatures near 100 °C and a weight loss due to the NH_4PA decomposition in a temperature range from 320 to 600 °C. This weight loss was used to determine the amount of NH_4PA adsorbed on each sample. Although the adsorption data obtained with this technique were semiquantitative, they provided a relative measure of the amount of NH_4PA adsorbed on the samples.

Rheological measurements

Steady state flow curves of FA slips were performed by measuring the steady shear stress value as a function of shear rate in the range of 0.5–542 s^{-1} using a concentric cylinder viscometer (Haake VT550, Germany) at 25 °C. A coaxial cylinder system with two gaps (sensor system NV Haake) was used. As soon as stationary conditions were reached at each shear rate, the shear rate increased in steps up to the maximum value and then decreased. The majority of the curves did not show hysteresis area. The relative viscosity $\eta_r = \eta_s/\eta_f$, where η_s and η_f are the viscosities of the suspension and the fluid medium (PVA + water + dispersant), respectively, was measured for 38 vol.% slips with 0.6 wt% NH_4PA and two PVA concentrations.

Slip casting and characterization of green samples

The slip casting process could be described as one-dimensional filtration, the slips flow unidirectionally through a cylindrical plaster mould. The casting rate of stabilized 38 vol.% slips with 0 and 0.5 wt% PVA was determined by measuring the thickness of the cake as a function of time. The thickness was measured for times $\geq$60 min, since for shorter times the error was high. The consolidated discs of diameter 2 cm were dried at room temperature and then at 100 °C.

The density of green compacts was determined by the Archimedes method using mercury displacement. The pore size distribution of green cakes was measured by mercury porosimetry (Porosimeter 2000 Carlo Erba, Italy). The diameter shrinkage upon drying of the consolidated green bodies was determined.

Sintering and characterization of sintered samples

Green cylinders were sintered in the temperature range 900–1500 °C, using a heating rate of 5 °C/min. The volumetric sintering shrinkage of the samples was measured; the bulk density was determined by water immersion (Standard Method ASTM C20). The microstructure of the sintered samples was observed on fracture surfaces using a scanning electron microscopy (SEM) (JEOL JSM 6360 LV, Japan).

Results and discussion

Powder characterization

The milling of the calcined powder reduced the particle size, thereby increasing the specific surface area from 1.79 to 17.77 m^2/g. The particle size distribution curve of the FA powder showed an unimodal distribution with a mean particle diameter of 0.37 μm.

The chemical composition of the calcined and FA powders is shown in Table 1. The chemical composition of the calcined powder indicated an excess of Ca and F with

Table 1 Chemical composition of different powders

Composition	Calcined	FA
SiO_2 (wt%)	0.24	0.24
Al_2O_3 (wt%)	0.14	0.14
Fe_2O_3 (wt%)	0.03	0.02
CaO (wt%)	57.6	56.5
MgO (wt%)	0.40	0.39
Na_2O (wt%)	0.28	0.12
K_2O (wt%)	0.02	0.02
Cr_2O_3 (wt%)	<0.01	<0.01
TiO_2 (wt%)	<0.01	<0.01
MnO (wt%)	0.01	0.01
P_2O_5 (wt%)	40.8	42.15
SrO (wt%)	0.02	0.02
BaO (wt%)	<0.01	<0.01
F (ppm)	>65000	37700
Ca/P atomic ratio	1.81	1.67

respect to the theoretical composition of $Ca_{10}(PO_4)_6F_2$. This was attributed to the excess of CaF_2 used in the preparation of fluorapatite (Eq. 1). Ca and F were removed during the milling and washing of the calcined powder, leading to an apatite with a Ca/P atomic ratio and a F content of 1.67 and 37700 ppm, respectively, which were close to the theoretical one. The milling and washing of the calcined powder also reduced the Na content. The average composition of the FA powder was found to be $Ca_{10}(PO_4)_6F_2$; the XRD patterns of FA corresponded to JCPDS # 15-0876; no additional phases were revealed (Fig. 1).

The FTIR spectra of the calcined and FA powders in the regions 450–1150 cm^{-1} and 3000–3800 cm^{-1} are presented in Fig. 2. The normal modes of the tetrahedral phosphate ion are: v_1, symmetric P–O stretching; v_2, OPO bending; v_3, P–O stretching; and v_4, OPO bending [16]. The fundamental vibrational modes of PO_4^{-3} tetrahedra of both samples were at 473 cm^{-1} (v_1); 965 cm^{-1} (v_2); 1047, 1097 cm^{-1} (v_3) and 572, 603 cm^{-1} (v_4) (Fig. 2a). The band near 3400–3500 cm^{-1} observed only for the FA, indicated adsorbed water on the particle surfaces during its milling (Fig. 2b). Besides, both spectra contained a band at 3540 cm^{-1} assigned to the F–O stretching. The intensity of this band and consequently the F content decreased after the aqueous milling of the calcined powder (Fig. 2b). This was in agreement with the chemical analysis.

FA surface reactivity

Figure 3 shows the mean particle diameter (d_{50}) as a function of pH for FA with 0 and 0.56 wt% NH_4PA. The FA could be dispersed at pH values >6; the d_{50} slightly

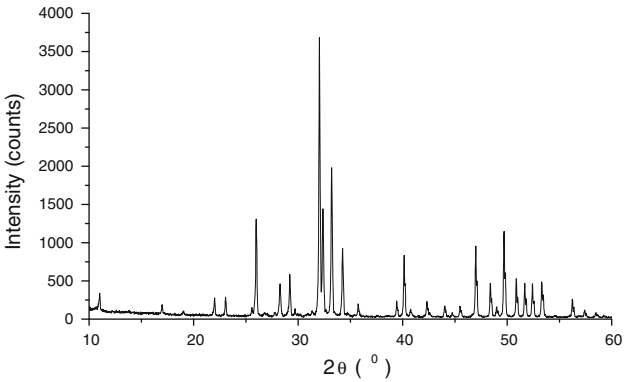

Fig. 1 XRD patterns of fluorapatite (FA). All peaks correspond to FA

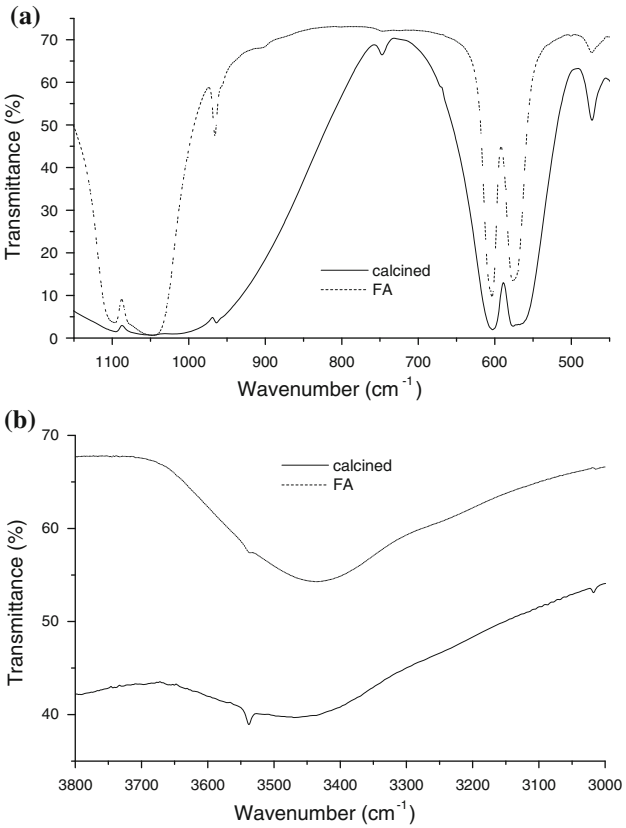

Fig. 2 FTIR spectra of the calcined and FA powders: **a** spectra over the 450–1150 cm^{-1} range, **b** spectra over the 3000–3800 cm^{-1} range

decreased with increasing pH from 6.5 to 9.9, reaching at this pH the lowest mean particle diameter of 0.75 μm. An important increase in the mean particle diameter was found with decreasing pH from 6 to 4; at pH ≤4 the d_{50} remained nearly constant.

The degree of aggregation of FA in aqueous dispersion was determined by the magnitude of the powder surface charge. At pH <6.5 a reduction in the electrostatic repulsion between particles was expected due to the strong

flocculation; the Van der Waals attraction forces were dominant and caused aggregation of the particles. In the pH range from 6.5 to 10 the particles became well dispersed indicating an increase in the electrostatic repulsion between particles. At pH $\leq$4 an increase in the repulsion between particles could be expected due to the high positive charge of the FA powder; however, the aggregation between particles still remained. This behaviour could be attributed to proton exchange reactions at the FA surface under strongly acidic conditions, which will be explained later.

The IEP of FA seemed to be about pH 6. Therefore, a negatively charged FA surface at pH >6 could be expected and a positively one at pH values lower than the IEP. Fluorapatite surfaces are thought to consist of two distinct surface groups $\equiv CaOH_2^+$ and $\equiv PO^-$ [17]. According to Chaïrat et al. [18], in acid to neutral conditions, apatite surface protonation proceeds via the formation of $\equiv CaOH_2^+$ leaving phosphate surface sites deprotonated. The Ca sites loss a proton in strongly alkaline solutions according to the following reaction:

$$\equiv CaOH_2^+ \rightarrow \equiv CaOH^0 + H^+ \quad (2)$$

The $\equiv CaOH_2^+$ concentration decreases with increasing pH and at pH >9.5 the $\equiv CaOH^0$ sites predominate [18].

The addition of NH_4PA shifted the curve towards lower pH values (Fig. 3). A well-dispersed FA suspension was found at pH $\geq$5, the mean particle diameter was nearly the same as the FA powder. At pH values lower than 4.5, flocculation occurred; however, aggregation of particles was lower than that observed in the absence of the dispersant. The ammonium polyacrylate dissociation according to the reaction:

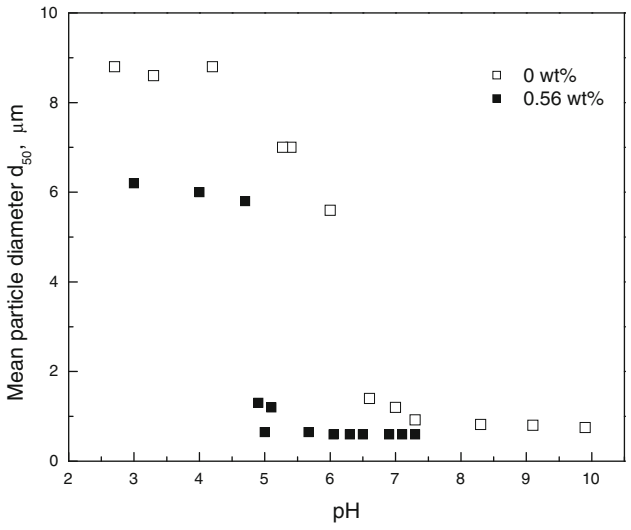

Fig. 3 Mean particle diameter (d_{50}) as a function of pH for FA with different NH_4PA contents: *open square* 0 wt%, *filled square* 0.56 wt%

$$RCOONH_4 \rightarrow RCOO^- + NH_4^+ \quad (3)$$

begins at pH >3.5; at pH values $\geq$8.5 the polymer charge is negative with the degree of ionization approaching 1 [9]. The $RCOO^-$ groups of the deflocculant were adsorbed at the positive $\equiv CaOH_2^+$ sites of the FA powder surface. The anionic polyelectrolyte was only slightly dissociated at pH <8.5; consequently, the electrostatic repulsion between the polyelectrolyte chains were of less importance and the steric contribution started to dominate.

Figures 4 and 5 show the pH of the suspensions and the Ca/P, F/P atomic ratios in the solid phase, respectively, as a function of time for the 1, 2 and 3 slips. The Ca/P and F/P atomic ratios during the dissolution differed from those of the dissolving stoichiometric apatite (Ca/P = 1.67 and F/P = 0.33), suggesting that the release of Ca and F were

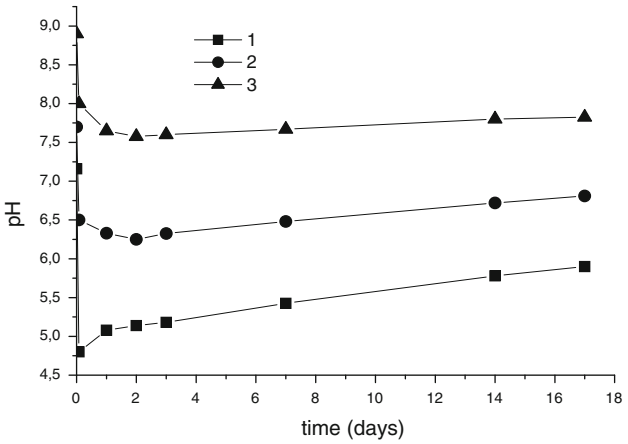

Fig. 4 pH as a function of time for three 10.4 vol% FA suspensions: (*1*) FA added to distilled water, (*2*) FA added to distilled water with 0.6 wt% NH_4PA at an initial pH 7.7 and (*3*) FA added to an aqueous solution having an initial pH of 8.9 with 0.6 wt% NH_4PA

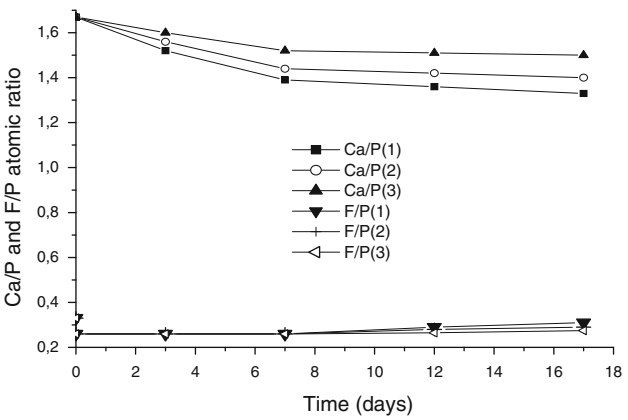

Fig. 5 Ca/P and F/P atomic ratio in the solid phase as a function of time for three 10.4 vol% FA suspensions: (*1*) FA added to distilled water, (*2*) FA added to distilled water with 0.6 wt% NH_4PA at an initial pH 7.7, and (*3*) FA added to an aqueous solution having an initial pH of 8.9 with 0.6 wt% NH_4PA

non-stoichiometric with respect to phosphorous for the three suspensions. For the 1 slip, an important adsorption of OH^- was found upon the FA introduction in aqueous solution, since at pH 7, which was close to the IEP of the FA powder, a high amount of positive surface groups still remained. As a result, the pH decreased to an acidic value up to a minimum of 4.8; along with OH^- adsorption a rapid removal of F from the near surface was found. Afterwards, the F/P atomic ratio remained nearly constant with increasing time up to 7 days, while the Ca/P atomic ratio decreased and the pH increased. Thus, after the initial preferential release of F relative to P, an exchange reaction between H^+ and Ca^{++} was involved in the uptake of H^+ by FA surfaces, in accordance with

$$Ca_{10}(PO_4)_6F_2 + 2x\ H^+ \leftrightarrow [Ca_{10-x}(HPO_4)_{2x}(PO_4)_{6-2x}]^{2+} + xCa^{++} + 2F^- \quad (4)$$

Chaïrat et al. [19] found that the Ca removal was coupled to phosphate hydrolysis and leaded to the formation of a protonated Ca-leached layer at FA surface. Thus, after the initial stage, proton consumption and release of Ca by Ca^{++}/H^+ exchange reaction occurred with increasing the pH of the solution and decreasing the Ca concentration in the solid phase accordingly. The same slope of the pH curve from 7 to 17 days indicated that the Ca^{++}/H^+ exchange reaction rate did not change. However, the slope of the Ca/P curve decreased and that of the F/P curve slightly increased. This was attributed to the detachment of phosphate anion together with Ca from the FA surface.

According to the results, a possible FA dissolution mechanism could consist in the following steps: (1) adsorption of OH^- at the positive surface groups and removal of F, (2) depletion of Ca and subsequent incorporation of protons, leading to the formation of a protonated Ca-leached layer; (3) detachment of phosphate tetrahedral together with Ca. This mechanism was in good agreement with that proposed by Dorozhkin [20] for the dissolution of apatite in acidic conditions.

The addition of FA to an aqueous solution with NH_4PA at pH 7.7 (2 slip) produced a lesser decrease in pH than that found for 1 slip. A minimum pH of 6.2 occurred at about 1 day (Fig. 4). The lower adsorption of OH^- was due to: (1) the FA powder had few positive surface groups at pH 7.7 since this pH was far from the IEP of the FA with NH_4PA (Fig. 3) and (2) the anionic polyelectrolyte slightly dissociated was adsorbed at some of the positive sites on the FA powder surface, leaving less ones for the OH^- adsorption. After 1 day the pH increased with increasing time with a lower slope than that found for the 1 slip. Simultaneously, the concentration of Ca decreased; however, the quantity of Ca remained at the FA surface was higher than that for the 1 slip through the whole dissolution time. The lower slopes of the pH and Ca/P curves were attributed to the decreasing FA dissolution rate with increasing pH (Eq. 4). The initial departure of F from the FA surface and the variation of F/P atomic ratio with time up to 7 days were similar to those found for the 1 slip. For longer time, the F/P atomic ratio of the solid phase slightly increased with a lower slope than that observed for the 1 slip, due to the lesser dissolution of P.

The introduction of FA in an aqueous solution with the pH adjusted at 8.9 with NH_4PA produced a scarcely lower decrease in pH than that observed for the 2 slip (Fig. 4). The $RCOO^-$ groups of the polyelectrolyte fully dissociated were adsorbed at some of the positive FA surface groups. However, as the amount of positive sites on the FA surface decreased with increasing pH, the powder had less positive groups at which the OH^- could be adsorbed. A minimum pH of 7.6 was found at about 1 day; for longer time the pH increased with a lower slope than those observed for the 1 and 2 slips, due to the decreasing in the Ca^{++}/H^+ exchange reaction rate with increasing pH. As a consequence, the Ca removal from the FA surface decreased with increasing pH; this determined that the slope of the Ca/P curve was lower than that observed for the 1 and 2 slips. Chaïrat et al. [18] demonstrated that the FA dissolution rate via Ca^{++}/H^+ exchange markedly decreased in weakly alkaline conditions. The F/P curve was similar to that of the 1 and 2 slips up to 7 days, for longer time the slope was scarcely lower than those of the 1 and 2 slips.

The FTIR-ATR spectra of unreacted FA, FA following its dissolution in an aqueous solution (1 powder), FA following its dissolution in an aqueous solution with 0.6 wt% NH_4PA at an initial pH 7.7 (2 powder), and FA following its dissolution in an aqueous solution with the pH initially adjusted at 8.9 with 0.6 wt% NH_4PA (3 powder) are presented in Fig. 6. In all the spectra the broad band at 3621 (Fig. 6a) was assigned to strongly adsorbed OH^- by coordination to $\equiv CaOH_2^+$ ions on the surface of the particles, whereas those at 960, 1017–1032 and 1090 cm^{-1} (Fig. 6b) to PO_4^{-3} group. The intensity of the 3621 cm^{-1} band and consequently the amount of OH^- adsorbed by the powder increased in the following order: FA, 3, 2 and 1 powders. This behaviour was consistent with the decrease in pH observed (Fig. 4) upon the FA introduction in the respective solutions.

The anti-symmetric PO_4^{-3} stretching band was observed at 1017 cm^{-1} on the FA powder and at 1020, 1023 and 1032 cm^{-1} on the 3, 2 and 1 powders, respectively. This peak shift was due to a change in the coordination environment of phosphate groups. The anti-symmetric PO_4^{-3} stretching band of octa-calcium phosphate ($Ca_8(HPO_4)_2(PO_4)_4{\cdot}5H_2O$) is located at 1038 cm^{-1} [21]. Thus, the shift of the peaks suggested protonation of surface P–OH groups and the subsequent incorporation of protons into the FA structure. Chaïrat et al. [19] observed a shift in the

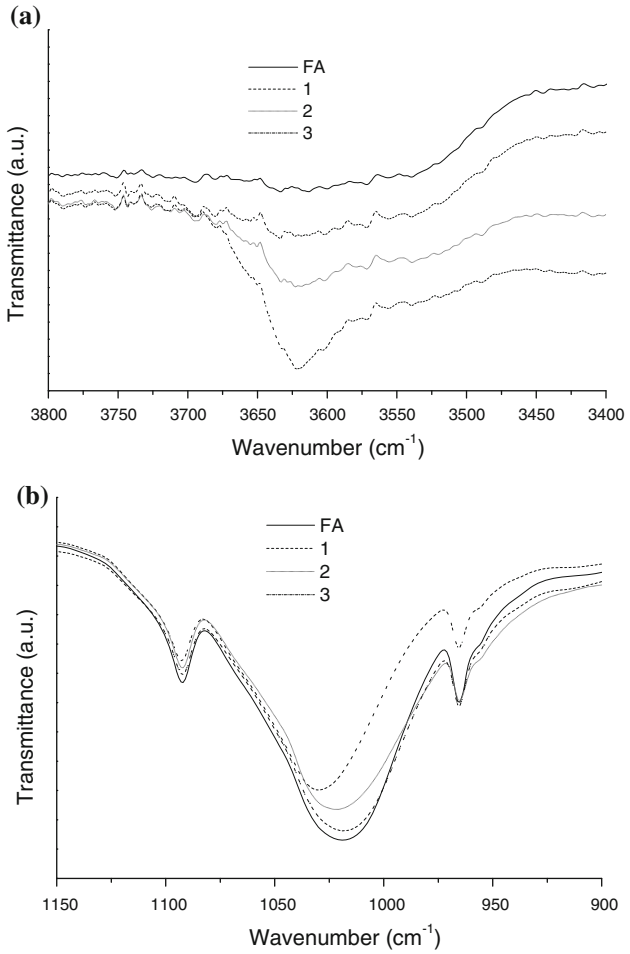

Fig. 6 FTIR-ATR spectra of unreacted FA, FA following its dissolution for 17 days in an aqueous solution (*1* powder), FA following its dissolution for 17 days in an aqueous solution with 0.6 wt% NH_4PA at an initial pH 7.7 (*2* powder), and FA following its dissolution for 17 days in an aqueous solution with the pH initially adjusted at 8.9 with 0.6 wt% NH_4PA (*3* powder): **a** spectra over the 3800–3400 cm^{-1} range, **b** spectra over the 1150–900 cm^{-1} range

phosphate stretching band position of FA dissolved in a pH 2 solution for 2 days. The greater shift of the 1 powder band indicated a greater incorporation of protons into the FA structure as a consequence of its dissolution in acidic conditions. The dissolution of FA in nearly neutral solutions (2 and 3 powders) resulted in a lower proton penetration into the surface lattice of FA. These results confirmed the pH measurements, a proton-Ca exchange reaction occurred at FA surface during its dissolution leading to the formation of a protonated Ca-leached layer. As a result, the FA surface composition in contact with aqueous solution was expected to be different from its bulk composition.

The Ca/P atomic ratio of the 3 and 1 powders were nearly 1.50 and 1.33, respectively. The Ca/P atomic ratio of the powder dissolved at the lower pH (1 powder), indicated that two calcium atoms were preferentially released from the FA surface during its dissolution for 17 days. This result and the FTIR spectra suggested that the leached surface layer might have a composition $[Ca_8(HPO_4)_4(PO_4)_2]^{+2}$ (Eq. 4).

The above mentioned results showed that: (1) the fluoride anions located at the surface have a high mobility. The initial release of F appeared to be independent of the initial pH of the solution and the presence of polymer. Thereafter, the F concentration in the solid phase remained nearly constant during the dissolution process; (2) the presence of NH_4PA and/or the increase in the initial pH of the solution markedly reduced the Ca^{++}/H^+ exchange reaction rate. The addition of FA to an aqueous solution with NH_4PA in weakly alkaline conditions (pH $\sim$9) produced the lowest decrease in pH, consequently the Ca removal and the up take of H^+ via proton–Ca exchange reaction were minimized; (3) the dissolved P in the final stage of the dissolution (after 7 days) decreased with increasing pH as a consequence of the lesser protons penetration into the surface.

Amount of NH_4PA adsorbed and powder characterization

Figure 7 shows the amount of NH_4PA adsorbed as a function of the amount of NH_4PA solution added at pH 8.9 for the FA powder. The amount of NH_4PA adsorbed increased with increasing amounts of NH_4PA solution added up to reaching an adsorption plateau at 0.6 wt% of NH_4PA solution added. This plateau corresponded to the adsorption saturation limit of the polyelectrolyte on the FA powder at pH 8.9. The adsorption curve did not follow the 100% adsorption line, thus the adsorption plateau was reached with an appreciable amount of NH_4PA remaining

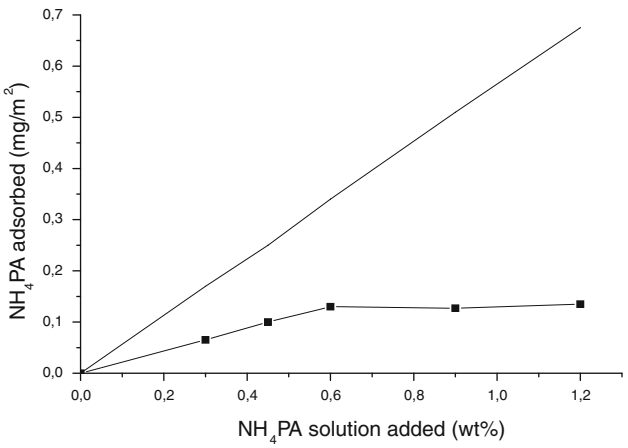

Fig. 7 Amount of NH_4PA adsorbed as a function of the amount of NH_4PA solution added at pH 8.9 for the FA powder. The *diagonal line* represents 100% of ammonium polyacrylate adsorption

in solution. At pH 8.9, the anionic polyelectrolyte was fully dissociated and the FA surface was negatively charged. The electrostatic repulsion at the surface imparts a barrier for adsorption which limited adsorption to low amounts [11]. However, the fact that adsorption occurred under these conditions indicated that there was a 'specific' or 'chemical' segment–surface interaction which overcompensated the repulsive electrostatic forces. Previous studies on alumina [9] and coated silicon nitride [22, 23] also found a detectable adsorption of anionic polyelectrolytes when the polyelectrolyte and the surface have the same charge sign.

During the aqueous colloidal processing of the FA powder with 0.6 wt% NH_4PA the pH of the suspension was adjusted at 8.9. At this pH, the Ca^{++}/H^{+} exchange reaction was markedly reduced, consequently a little change in the surface composition of the FA powder could be expected. Figure 8 shows the FTIR-ATR spectra of the FA powder before and after its colloidal processing in an aqueous solution at pH 8.9 with NH_4PA. A similar intensity and position of the PO_4^{-3} bands (Fig. 8b) and a similar OH^{-} adsorption (Fig. 8a) were detected. This confirmed that the aqueous colloidal processing of FA with NH_4PA at pH 8.9 did not change the coordination environment of phosphate groups.

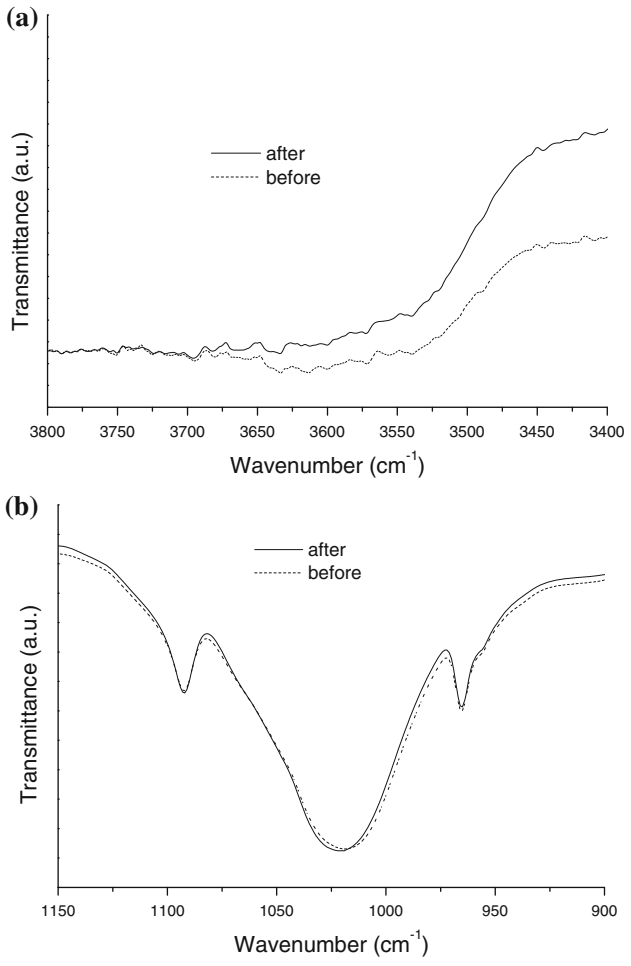

Fig. 8 FTIR-ATR spectra of the FA powder before and after its colloidal processing in an aqueous solution at pH 8.9 with NH_4PA: **a** spectra over the 3800–3400 cm^{-1} range, **b** spectra over the 1150–900 cm^{-1} range

Rheological properties

Figure 9 shows the flow curves of viscosity versus shear rate as a function of the amount of NH_4PA solution added at pH 8.9 for 40 vol% FA slips. All the curves showed a yield stress and the viscosity values were strongly dependent on the shear rate; thus, the suspensions exhibited a pseudoplastic behaviour. The measured flow curves were satisfactorily fitted with the Casson model ($R = 0.99$). The Casson model equation is:

$$\tau^{1/2} = \tau_0^{1/2} + (\eta_p \gamma)^{1/2} \quad (5)$$

where τ is the shear stress, γ is the shear rate, τ_0 is the yield stress and η_p represents the limiting viscosity at a high shear rate range. The τ_0 and η_p constants of the model could be used to represent the rheological properties of the slips.

The particles in a flocculated suspension form floc groups or a network, because of the mutual attraction between particles, and the yield value τ_0 of the Casson model could be used as a parameter that indicated the degree of aggregation and consequently the degree of flocculation. The η_p value becomes equal to the viscosity when $\tau_0 \rightarrow 0$.

Figure 10 shows the effect of the amount of NH_4PA solution added on the τ_0 and η_p values. For the FA slip with 0.3 wt% NH_4PA the amount of NH_4PA adsorbed was

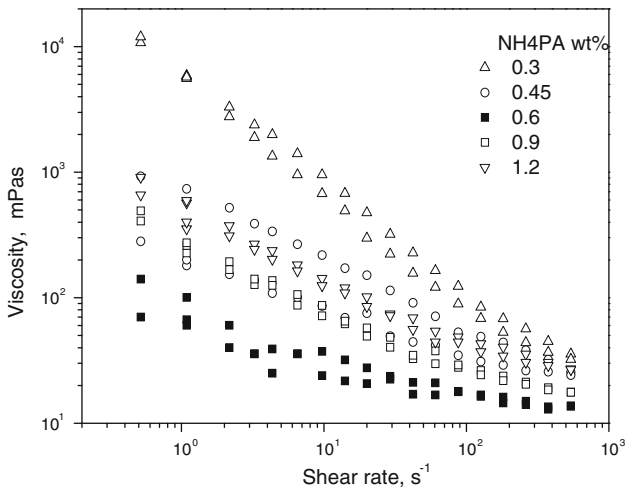

Fig. 9 Flow curves of viscosity versus shear rate as a function of the amount of NH_4PA solution added at pH 8.9 for 40 vol% FA slips

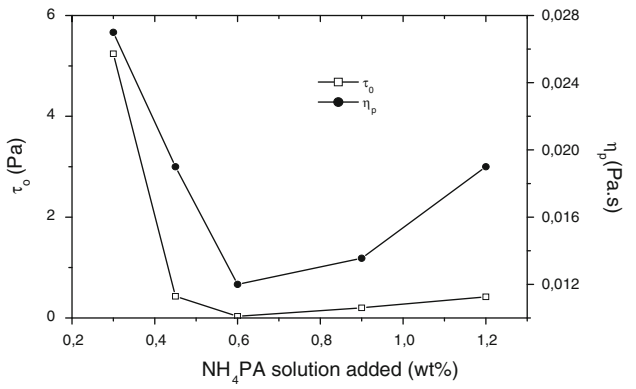

Fig. 10 Effect of the amount of NH_4PA solution added on the τ_0 and η_p values for 40 vol% FA slips

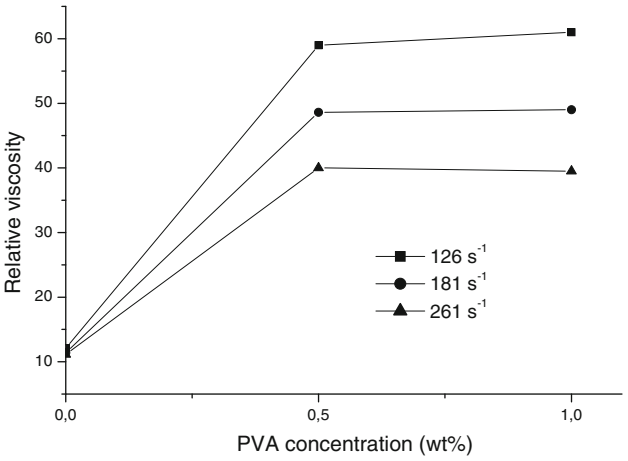

Fig. 11 Relative viscosity as a function of the PVA concentration for 38 vol.% suspensions stabilized with 0.6 wt% NH_4PA at three different shear rates

lower than the adsorption saturation limit of the polyelectrolyte on the FA surface (Fig. 7), the suspension was flocculated and this condition resulted in high τ_0 and η_p values. The incomplete adsorption of the polyelectrolyte resulted in lower electrostatic repulsion between particles, thereby forcing particles together. Further additions of NH_4PA resulted in a decrease in the τ_0 and η_p values. The adsorption of the negatively charged polyelectrolyte enhanced the negative surface charge of the FA powder. In addition, at pH 8.9 the electrostatic repulsion between the charged carboxylate groups impedes the accumulation of groups at the surface; the polyelectrolyte adsorbs in a stretched-out configuration which results in long-range steric interactions of the NH_4PA at the solid–liquid interface [24]. Thus, the adsorbed molecules increased the electrosteric repulsion between particles, thereby decreasing the slip viscosity.

For 0.6 wt% NH_4PA the viscosity and consequently τ_0 and η_p attained the minimum values. As the adsorption coverage increased (Fig. 7) the negative surface charge density and the electrostatic repulsion between particles increased accordingly and, eventually, attained a level at 0.6 wt% NH_4PA that was strong enough to overcome the Van der Waals forces. At this NH_4PA concentration the suspension was dominated by repulsive forces, thus, it was stabilized. The viscosity at 400 s^{-1} was reduced to a low value of about 13 mPa s. As the NH_4PA addition increased over 0.6 wt% the slips changed from being well stabilized to weakly flocculated. The increase in the ionic strength due to the presence of a large amount of free polymer in solution decreased the negative surface charge of the FA powder due to the large compression of the double layer [25], which produced the increase in the slip viscosity. As a consequence an increase in the τ_0 and η_p values was found.

As we have mentioned, the addition of PVA can change the rheology of a dispersant stabilized suspension significantly [13]. Figure 11 represents the relative viscosity at three different shear rates as a function of the PVA concentration for 38 vol.% suspensions stabilized with 0.6 wt% NH_4PA. At the three shear rates examined, the relative viscosity increased as the PVA concentration increased from 0 to 0.5 wt%; thereafter, the relative viscosity remained virtually unchanged. The increase in the relative viscosity was approximately four times as the PVA concentration increased from 0 to 0.5 wt%. The increase in the viscosity with the addition of PVA suggested that the PVA produced a flocculation of the FA particles. The degree of flocculation was more pronounced for the PVA concentration range between 0 and 0.5 wt%. Above 0.5 wt% PVA, there was little change in the degree of flocculation. Khan et al. [13] found a similar behaviour when PVA was added to stabilized alumina suspensions. They found that PVA did not adsorb to any measurable extent, on the alumina particles, therefore they explained that the aggregation of alumina particles was caused by a depletion flocculation process when PVA was added to the suspension.

The addition of PVA to stabilized FA suspensions might cause depletion flocculation, whereby the concentration of the non-adsorbing free PVA was effectively reduced between the particles, and the higher concentration outside the particle–particle approach zone, exerted an osmotic pressure causing the particles to flocculate. Thus, the addition of PVA promoted aggregation of particles by a depletion flocculation mechanism.

Casting rate of suspensions with and without PVA

Slip casting is the formation of a consolidated layer, or cake, on the surface of a porous body [26]. During this process, a dry porous mould contacts a suspension and the

porous surface is wetted by the suspension. The capillary suction caused by the porous mould drives ceramic particles to concentrate at the mould–suspension boundary, and a wet cake is formed if the particles cannot enter into the pores [26]. In this capillary filtration, the driving force behind the fluid flow is the capillary suction pressure of the mould [26]. Fluid flow through the consolidated layer and into the porous body is governed by the Darcy's law, which express the variation of the layer thickness, h, as a function of time, t. When the permeability of the mould is much larger than that of the cake [14], the equation for the formation of the wet cake can be expressed as

$$h = 2(\varepsilon_n \gamma K t/\eta \alpha R_n)^{1/2} \quad (6)$$

where K is the permeability of the wet cake, η is the viscosity of the liquid, R_n is the pore radius of the mould and ε_n its porosity, γ represents the surface tension of the liquid in the pores of the mould and α is defined as $(\varphi_0/\varphi) - 1$ (φ_0 and φ are the volume fraction of particles in the suspension and in the wet cake, respectively). This equation shows that when the suspension and the mould are fixed, the cake thickness square increases linearly with the time. It also implies that the structures of the porous mould and the wet cake, and the properties of the suspension have close relation to the cake formation process. In this work, the porosity and the pore diameter of the mould were fixed, therefore the cake formation rate depended on the pore structure of the wet cake and the viscosity of the fluid.

Figure 12 shows the layer thickness square as a function of time for stabilized 38 vol.% slips with 0 and 0.5 wt% PVA. The linear relation of the two series of data demonstrated that they were in good agreement with the model described above. At the beginning (60 min), a greater casting rate of the slip without PVA with respect to that with PVA was found, resulting in an increase of the layer thickness. This was attributed to the lower viscosity of the fluid without PVA which increased the initial liquid flow through the porous mould. Once the cake was growing ($t > 60$ min), the casting rate of the slip without PVA was significantly lower resulting in a reduction of the layer thickness at a given time.

In order to explain the difference between the h^2 versus t curves the pore structure of the resultant green cakes were examined. Figure 13 shows the cumulative micropore volume by mass unit versus pore radius curve of cakes obtained from slips with 0 and 0.5 wt% PVA. An unimodal distribution of pore sizes was observed for both samples, the most frequent pore radius were 0.02 and 0.03 μm for the cakes produced from slips with 0 and 0.5 wt% PVA, respectively. A greater volume of pores was found for the cake obtained from the slip with PVA (Fig. 13). Thus, the volume and size of the most frequent pore radius within the cake increased when the slip with high viscosity was cast. These greater porosity and pore size increased the permeability of the cake, thereby increasing the casting rate (Eq. 6). The casting rate of the slip without PVA was significantly reduced as there were fewer paths for liquid flow within the cake. Thus, for $t > 60$ min when the cake was growing, the casting rate was governed by its permeability. The higher casting rate of slips with PVA would be beneficial in the dip coating process to produce thicker layers on a porous substrate immersed in the slurry.

Table 2 lists the relative viscosity values of the suspensions with 0 and 0.5 wt% PVA at a shear rate of 126 s^{-1}, together with the density and percentage diameter shrinkage upon drying of the consolidated green bodies. The lower viscosity values of slips without PVA produced green bodies with higher densities; this was consistent with the lower volume of pores found after slip casting (Fig. 13). In these slips, the particles could pack in an ordered way due to the repulsive forces existing between them, resulting in high green densities of slip cast bodies.

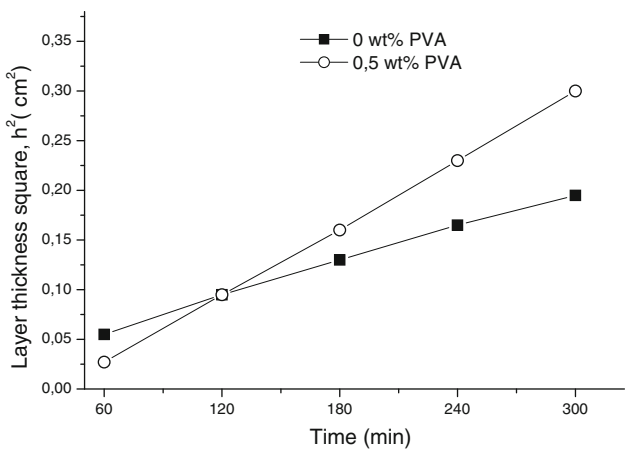

Fig. 12 Layer thickness square as a function of time for stabilized 38 vol.% slips with 0 and 0.5 wt% PVA

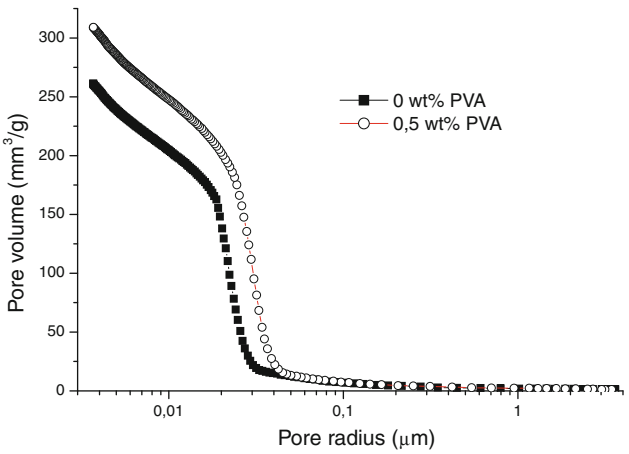

Fig. 13 Cumulative micropore volume by mass unit versus pore radius curve of cakes prepared from slips with 0 and 0.5 wt% PVA

Table 2 Relative viscosity of 38 vol.% stabilized suspensions with 0 and 0.5 wt% PVA and properties of the consolidated green bodies

Sample	Slurry relative viscosity (at $\gamma = 126\ s^{-1}$)	Green density (%TD)	Diameter shrinkage upon drying (%)
0 wt% PVA	11.8	61.5	0.4
0.5 wt% PVA	58.8	57.0	0.1

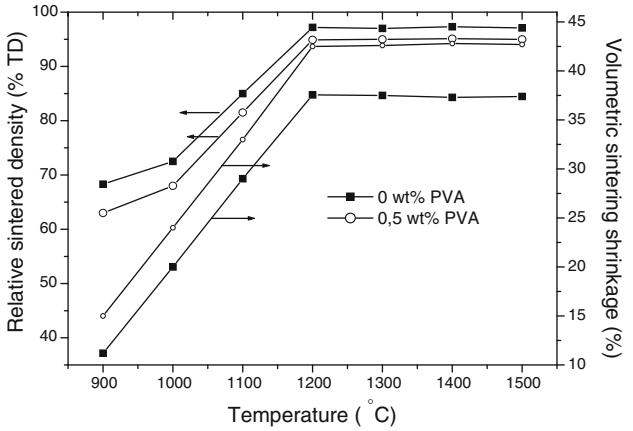

Fig. 14 Relative sintered density and volumetric sintering shrinkage of samples obtained from slips with 0 and 0.5 wt% PVA as a function of temperature after sintering for 1 h

The addition of PVA promoted aggregation of particles increasing the slip viscosity; consequently, compacts with lower green densities were obtained. Green bodies obtained using slips without PVA exhibited higher shrinkage values upon drying than those produced from slips with PVA. The closeness of the particles forming fine pores in the green bodies prepared from slips without PVA exerted a high suction pressure, the driving force for drying shrinkage, equivalent to an external applied pressure that promoted shrinkage. Nevertheless, the drying shrinkage was very low due to the high solids loading of the starting suspensions. The results demonstrated that the viscosity of the suspensions (i.e. degree of particle dispersion) greatly affected the growth rate of the cake and the density of the resultant green bodies.

Figure 14 shows the relative sintered density and the volumetric sintering shrinkage of samples obtained from slips with 0 and 0.5 wt% PVA as a function of temperature after sintering for 1 h. For both samples, the sintered density increased with increasing temperature, reaching nearly full densification at 1200 °C. Thus, the porosity was not further eliminated for temperatures higher than 1200 °C. Figure 15 shows SEM images of samples prepared from slips with 0.5 wt% PVA sintered at different temperatures. Densification, thus, a markedly reduction in the porosity with increasing sintering temperature could be

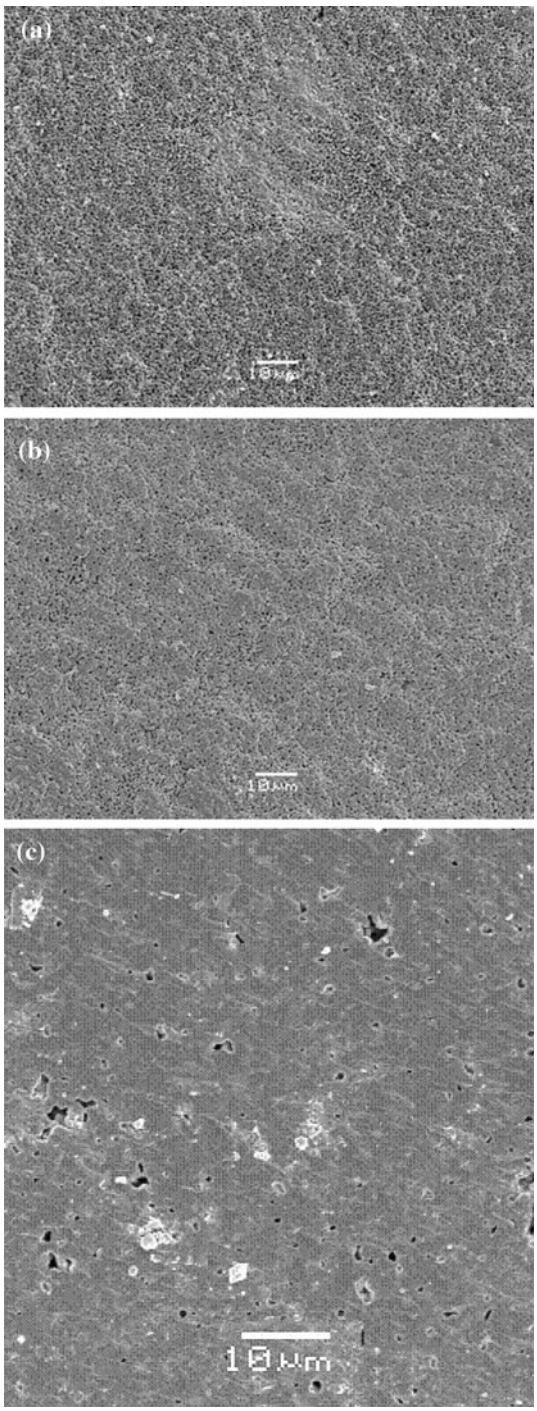

Fig. 15 SEM micrographs of samples prepared from slips with 0.5 wt% PVA sintered at different temperatures: **a** 900 °C, **b** 1100 °C, **c** 1200 °C

observed up to 1200 °C; at this temperature the sample was nearly fully densified. Some large pores were not eliminated by sintering at 1200 °C (Fig. 15c). Sintered densities of 95% and 97% of the theoretical density (TD) were achieved for the bodies obtained using slips with 0.5 and 0 wt% PVA, respectively. There was a close relation

between green and sintered densities, the less dense materials produced from slips with PVA were attributed to the less particle packing achieved in the green bodies (Table 2).

The sintering shrinkage behaviour was in accordance with the relative sintered density versus temperature curves. Thus, an important increase in the volumetric shrinkage upon sintering was found up to 1200 °C, then it did not change with further increasing of the sintering temperature. The sintering shrinkage values of the samples prepared from slips with PVA were higher than those of the slips without PVA throughout the whole range of temperatures, due to the lower green densities of cast samples.

Conclusions

The surface reactivity of fluorapatite in an aqueous solution with and without dispersant was investigated. An initial release of F anions located at the surface was found, which was not dependent on the initial pH of the solution and the presence of dispersant. The increase in the initial pH of the solution above 7 and/or the presence of NH_4PA markedly reduced the Ca^{++}/H^{+} exchange reaction rate. The addition of FA to an aqueous solution with NH_4PA in weakly alkaline conditions (pH $\sim$9) produced the lowest decrease in pH, consequently the Ca and P removal and the up take of H^{+} via proton-Ca exchange reaction were minimized.

The aqueous colloidal processing of FA with NH_4PA at pH 8.9 did not change the coordination environment of phosphate groups. The minimum viscosity of 40 vol.% slips at pH 8.9 occurred at 0.6 wt% of NH_4PA added. At this concentration, the saturation adsorption limit of fully dissociated NH_4PA was reached providing a high degree of particle stabilization.

The addition of 0.5 wt% PVA to a well-stabilized FA slip caused an aggregation of particles, thereby increasing the slip viscosity. The increase in viscosity was probably due to a depletion flocculation mechanism. The viscosity became nearly constant in the 0.5–1 wt% PVA concentration range.

The high viscosity values of the slips with PVA promoted the formation of more porous green microstructures and lower densities of slip cast bodies. The greater permeability of these cakes also increased the casting rate. As a consequence, these green bodies exhibited lower densities and higher shrinkage after sintering.

References

1. Weiner S, Wagner HD (1998) Ann Rev Mater Sci 28:271
2. Vallet-Regí M, González-Calbet JM (2004) Prog Solid State Chem 32:1
3. Dorozhkin SV (2009) Materials 2:1975
4. Suchanek W, Yoshimura M (1998) J Mater Res 13:94
5. Hench LL (1991) J Am Ceram Soc 74(7):1487
6. Kim H-W, Lee S-Y, Bae C-J, Noh Y-J, Kim H-E, Kim H-M, Ko JS (2003) Biomaterials 24:3277
7. Kim H-W, Yoon B-H, Koh Y-H, Kim H-E (2006) J Am Ceram Soc 89(8):2466
8. Chaari K, Bouaziz J, Bouzouita K (2005) J Colloid Interface Sci 285:469
9. Cesarano J III, Aksay IA, Bleier A (1988) J Am Ceram Soc 71(4):250
10. Cesarano J III, Aksay IA (1988) J Am Ceram Soc 71(12):1062
11. Guldberg-Pedersen H, Bergström L (2000) Acta Mater 48:4563
12. Zhang J-X, Jiang D-L, Tan S-H, Gui L-H, Ruan M-L (2001) J Am Ceram Soc 84(11):2537
13. Khan AU, Briscoe BJ, Luckham Pf (2000) Colloids Surf A 161:243
14. Gu Y, Meng G (1999) J Eur Ceram Soc 19:1961
15. Hampton JHD, Savage B, Drew RAL (2005) J Am Ceram Soc 71(12):1040
16. Bhatnagar VM (1971) Can J Chem 49:662
17. Rodenas LG, Palacios JM, Apella MC, Morando PJ, Blesa MA (2005) J Colloid Interface Sci 290:145
18. Chaïrat C, Schott J, Oelkers EH, Lartigue J-E, Harouiya N (2007) Geochim Cosmochim Acta 71:5901
19. Chaïrat C, Oelkers EH, Schott J, Lartigue J-E (2007) Geochim Cosmochim Acta 71:5888
20. Dorozhkin SV (1997) J Cryst Growth 182:133
21. Berry EE, Baddiel CB (1967) Spectrochim Acta A 23:1781
22. Albano MP, Garrido LB (1998) J Am Ceram Soc 81(4):837
23. Albano MP, Garrido LB (2004) Colloids Surf A 248:1
24. Liu D, Malgham SG (1996) Colloids Surf A 110:37
25. Albano MP, Garrido LB, Garcia AB (2001) Colloids Surf A 181:69
26. Tiller FM, Tsai C (1986) J Am Ceram Soc 69(12):882